Analyzing Urban Spatial Connectivity Using Night Light Observations: A Case Study of Three Representative Urban Agglomerations in China

Xia Zhao, Xi Li, Yuyu Zhou, and Deren Li

***Abstract*—Urban connectivity information is important for regional planning of sustainable development goals. However, there are still challenges in deriving the spatial connectivity relationship among urban areas. The nighttime light data measure anthropogenic phenomenon remotely and can be seen as a unique source for monitoring urban spatial expansion and human activities. This study presents an object-based approach for investigating spatial connectivity among urban patches by incorporating Suomi National Polar-Orbiting Partnership Visible Infrared Imaging Radiometer Suite Day/Night Band and land use data collected in 2015. A graph-based method is used to construct connectivity networks and explore spatial patterns considering both quantity and quality of connections in three vibrant urban agglomerations in China, namely, Jing-Jin-Ji (JJJ), Yangtze River Delta (YRD), and Pearl River Delta (PRD) megaregions. Results indicate that networks follow a power law distribution according to cumulative degree distributions. A closer connectivity relationship exists among urban patches in PRD, with a relatively high-intensity connection ratio and a mean degree of 4.5, compared with YRD and JJJ. Block-like connections are observed in core areas of all urban agglomerations (UAs), and single-tree connections are found in peripheral areas. This article implies a significant inequality in the regional development and hub–spoke structures with hubs of provincial capitals and municipalities. Our proposed framework is transferrable for the analysis of connectivity relationship in other regions, and the outcome can contribute to the study of evolution of UAs and bring insights to policymakers for sustainable development at regional level.**

***Index Terms*—National Polar-Orbiting Partnership Visible Infrared Imaging Radiometer Suite Day/Night Band (NPP-VIIRS), Nighttime light (NTL), remote sensing, urban agglomeration, urban connectivity.**

Manuscript received November 17, 2019; revised February 16, 2020 and March 2, 2020; accepted March 7, 2020. Date of publication March 17, 2019. This work was supported in part by the Open Fund of Key Laboratory of Geospatial Technology for the Middle and Lower Yellow River Regions (Henan University), Ministry of Education under Grant GTYR201804 and in part by the National Natural Science Foundation of China under Grant 41771386. *(Corresponding authors: Xi Li; Yuyu Zhou.)*

Xia Zhao is with the State Key Laboratory of Information Engineering in Surveying, Mapping and Remote Sensing, Wuhan University, Wuhan 430079, China, and also with the Department of Geological and Atmospheric Science, Iowa State University, Ames, IA 50010 USA (e-mail: zhaoxia2015@whu.edu.cn).

Xi Li is with the State Key Laboratory of Information Engineering in Surveying, Mapping and Remote Sensing, Wuhan University, Wuhan 430079, China, and also with the Key Laboratory of Geospatial Technology for the Middle and Lower Yellow River Regions (Henan University), Ministry of Education, Kaifeng 475004, China (e-mail: lixi@whu.edu.cn).

Yuyu Zhou is with the Department of Geological and Atmospheric Science, Iowa State University, Ames, IA 50010 USA (e-mail: yuyuzhou@iastate.edu).

Deren Li is with the State Key Laboratory of Information Engineering in Surveying, Mapping and Remote Sensing, Wuhan University, Wuhan 430079, China (e-mail: drli@whu.edu.cn).

This article has supplementary downloadable material available at http://ieeexplore.ieee.org, provided by the authors.

Digital Object Identifier 10.1109/JSTARS.2020.2980514

I. Introduction

URBANIZATION is a global and complicated phenomenon that simultaneously involves the migration of population from rural to urban, the shift of the economy from agriculture to manufacturing and service industries, and the transformation of natural land surfaces into artificial urban landscapes [1]–[3]. The ongoing urbanization process has increased the integration of urban landscapes and not only the continuously aggregated metropolitan areas, but also the connections among cities [4]. This process generates urban agglomerations (UAs) worldwide. The UA is more than a simple collection of cities, and it is also the inner integration of people, physical structures, economics, and information; it is shaped by one or two leading cities and several adjacent cities [5]. The connectivity relationship among cities plays an important role in acknowledging regional development and provides knowledge regarding the evolution of UAs [6]–[8].

Previous studies of urban relationship can be divided into three major categories regarding data types, namely, transportation data, population, and information flows. The first category mostly refers to airlines [9], [10], railways [11], and road networks [12]. The second category includes commuting data [13], migration flows [14], [15], and trip networks derived from social media data [16]. The third category typically uses the Baidu Index that represents the mutual focus of users among cities [17] and Sina microblog [18]. Nonetheless, identifying the relationship among urban areas is a challenging problem from several aspects. First, no single variable can measure the actual connectivity relationship among cities [4]. For example, although many cities do not have airports, such as Suzhou in China, they are still well-connected with other cities. Second, the basic units of these analyses only focus on the administrative divisions at the city and provincial scales. Consequently, the internal connections of urban patches belonging to the same city are not shown, and the strongest connections of urban aggregated areas, such as junction urban areas that belong to different divisions, are neglected. Third, these studies suffer from the labor-intensive processing of collected data and are prone to

uncertainties. Thus, new data sources are urgently needed for urban connectivity relationship.

Remote sensing technology has been demonstrated as an effective tool for monitoring land surface conditions across various spatial scales with a continuous spatial coverage and diverse data reserves [19]–[24]. For example, nighttime light (NTL) observations record light emissions from the Earth's surface at night. Many studies have documented the high correlation of NTL with economics [25]–[28], population density and carbon emissions [29]–[32], and freight traffic [33], [34]. Various researchers have reported their success in mapping urban areas derived from the sole input of NTL data [21], [35]–[39]; however, only a few studies have explored the relationship among urban areas using NTL data.

The existing studies using NTL data to explore the spatial relationship of urban areas can be grouped into three categories. The first is based on the spatial proximity relationship of urban patches. For example, Yu *et al.* [40] distinguished the major UAs in China by examining the spatial cluster relationship of urban objects derived from the Defense Meteorological Satellite Program (DMSP) NTL data. The second involves analogizing NTL images as the contiguous surface representing the intensity of human activities. For example, Chen *et al*. [41] explored the functions and accessibility of urban areas in Shanghai by analyzing the concentration levels of human activities using Visible Infrared Imaging Radiometer Suite (VIIRS) Day/Night Band (DNB) data. Wu *et al.* [42] proposed a method for detecting the hierarchical relationship of urban areas and successfully experimented in 32 major cities in China. Third, Small *et al*. [43], [44] pointed out the great potential of VIIRS DNB data in detecting the vast spatial network among human settlements with the capability of resolving lighted road networks.

Investigating the spatial connectivity relationship of urban areas based on NTL data still faces challenges. First, although DMSP NTL data can be used to derive urban extents, these observations exert a blooming effect, which makes the detected urban areas considerably larger than the real built-up areas [21], [45], and this issue inevitably influences the spatial proximity of urban areas. Second, although studies have well detected the hierarchical relationship of urban areas by analogizing NTL data as the intensity surface of human activities, these studies focus only on the interior urban areas of a city. Third, the spatial connectivity relationship of urban areas in these studies are only characterized through rank-size distribution by setting various segmentation thresholds.

In this article, we propose an object-based approach for detecting spatial connections among urban patches based on NTL data and explore urban connectivity networks using a graph-based method. The remainder of this article is organized as follows. Section II describes the related data set and the experiment areas. In Section III, we provide an overview of the study procedure, including the connectivity detection method, the graph-based analysis method, and the centrality measures of urban patches. Section IV discusses the visualization results and the quantitative analysis results of urban connectivity relationship in the context of UAs. Finally, Section V concludes this article.

II. Study Area and Data

A. Study Area

This study focuses on the three national-level UAs in China, namely, Jing-Jin-Ji (JJJ, with 13 cities), Yangtze River Delta (YRD, with 42 cities, including Hefei Province), and Pearl River Delta (PRD, with 11 cities, including Hong Kong and Macau) (see Fig. 1) [46], which have experienced the fastest population growth and rapid urbanization over recent decades. The JJJ region is located in the Northern China Plain, with two municipalities (Beijing and Tianjin) as leading cities. YRD is situated in the alluvial plain of the Yangtze River, with Shanghai as the center and Nanjing, Hangzhou, and Hefei as the subcenters. PRD is the confluence of three large rivers endowed with geographical advantage, with Guangzhou, Shenzhen, and Hong Kong as leading cities. Their basic information is provided in Table I. These regions have continued to be prosperous and energetic since the reform and opening of China.

Although three UAs occupy only 5.1% of the national territory, they account for nearly 30.4% of China's total population and generate 42.5% of the total gross domestic product (GDP), nearly 30.1% of total passenger traffic and 32.9% of total freight traffic according to 2016 National Statistics Yearbook of China [48]. These statistics indicate that the most frequent, highly demanding physical and economic movements occur in these regions. The NTL images of the three UAs in 2015 are shown in Fig. 1(b)–(d).

B. Data and Preprocessing

The annual product of the version 1 of nighttime VIIRS DNB cloud-free composites tile 3 (75°N/60°E to 0°N/18°0E) from [49] in 2015 is used in this article. VIIRS DNB collects information across a single wide spectral band that covers the wavelength range of 0.5–0.9 μm, with a spatial resolution of 15 arc-second. The annual DNB data are filtered to exclude data impacted by stray light, lightning, lunar illumination, and cloud cover [50]. In the annual composite, settlements and their interconnectivity can be clearly observed and, thus, the connectivity among urban areas can be detected [43]. The image used for this article is projected to the North Albers Equal Area Conic Projection referencing World Geodetic System 84 datum and resampled to a spatial resolution of 500 m using the nearest sampling method.

The land use data used in this study are from the Resources and Environment Data Center of the Chinese Academy of Sciences [51]. This product has been widely used and evaluated in previous studies [21], [52], [53]. It was derived from the visual interpretation of Landsat Enhanced Thematic Mapper Plus remotely sensed images with a spatial resolution of 1 km. Pixels are categorized into a small set of nominal values to delineate how land appears or is being used. With regard to built-up land use, the classification system includes three types—urban, rural, and other built-up areas. In this article, only urban built-up areas are selected to depict urban spatial extents. The image

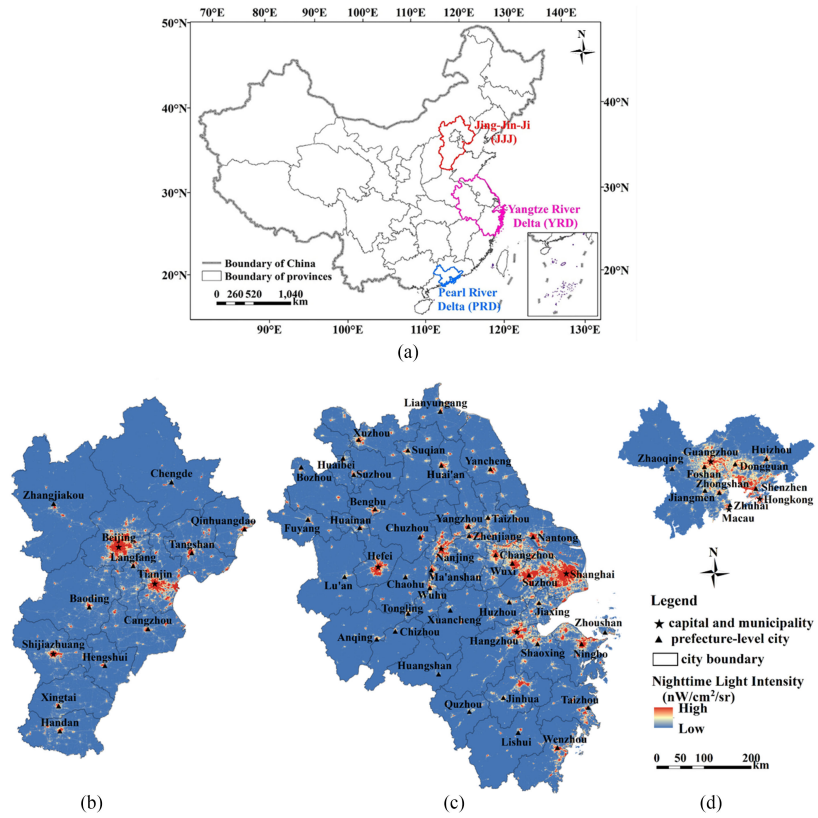

Fig. 1. Study areas of three UAs (a) and NTL maps of JJJ (b), YRD (c), and PRD (d) in 2015.

TABLE I
INFORMATION OF THREE UAs (JJJ, YRD, AND PRD)

UA	Area (million km^2)	GDP (billion RMB)	Per capital GDP (RMB)	City number	Municipality and province	Core city [a]	
JJJ	0.216	6935.9	84904.0	13	Beijing Tianjin Hebei	Beijing Tangshan	Tianjin Baoding
YRD	0.359	16013.2	76357.7	42	Shanghai Jiangsu Zhejiang Anhui	Shanghai Suzhou Changzhou Yangzhou Nantong Ningbo Jiaxing Zhoushan	Nanjing Wuxi Zhenjiang Taizhou (JS) Hangzhou Huzhou Shaoxing Taizhou (ZJ)
PRD	0.056	5916.3	101433.4	11	Part of Guangdong	Guangzhou Zhuhai Jiangmen Huizhou Zhongshan Macau	Shenzhen Foshan Zhaoqing Dongguan Hong Kong

[a]JS = Jiangsu province; ZJ = Zhejiang province. The definition of "core city" is based on [47].

is preprocessed to be consistent with VIIRS DNB data with a spatial resolution of 500 m.

III. METHODOLOGY

In this article, our proposed workflow of urban connectivity analysis consists of the following three steps (see Fig. 2).

Step 1: Detection of spatial connectivity among urban patches based on VIIRS data and the urban built-up areas (see Section III-A).

Step 2: Construction of the weighted spatial network based on the graph theory (see Section III-B).

Step 3: Calculation of network metrics to characterize the network properties (see Section III-C).

A. Detection of Spatial Connectivity Among Urban Patches

1) Identifying Urban Patches: Urban areas extracted from the land use data are delineated as urban patches. Each urban patch consists of spatially contiguous urban pixels. Different

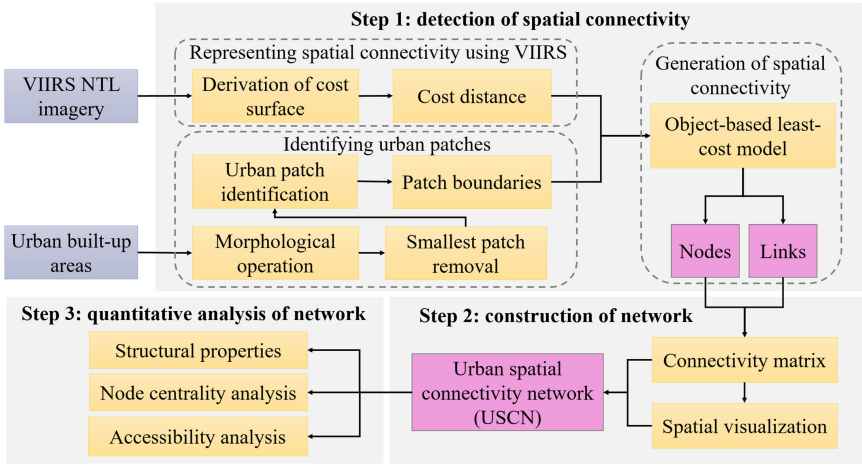

Fig. 2. Flowchart of the objected-based urban connectivity analysis using VIIRS NTL.

from previous urban network studies using transportation data and constrained within administrative units, the basic analysis units of urban patches in this study are more reasonable. The distribution of these urban patches is not entirely consistent with administrative divisions. Small urban patches may correspond to a county or a separated urban district of a city, and large urban patches may cover an entire city or multiple adjacent cities in metropolitan areas. Patches may also span several counties or urban districts. Thereafter, two types of morphological operations, namely, filling and closing, are utilized to fill small holes and smooth urban patch boundaries. The filling operation fills all holes in the binary images (urban built-up areas are denoted as 1, nonbuilt-up are 0). For the closing operation, we use a flat and disk-shaped window with a search radius 3 [40]. Then, we use a recursive connected-region labeling algorithm to definitely mark urban patches on the basis of the spatial four-connectivity of foreground urban pixels [40]. Urban built-up areas tend to have small and even single-pixel patches, and these small urban patches have a small impact on the connectivity analysis of a network while they can significantly increase the computation. Therefore, we define and mask out small urban patches on the basis of urban patches' rank-size distribution [54] [see Supplementary Fig. S1(a)]. The distributions of scatter points show obvious breaks along the value of 2. We selected urban patches greater than the value 2, and the finally selected urban patches accounted for more than 90% of total areas in each UA, including all administrative located areas and main human activities crowed areas [see Supplementary Fig. S1(b) and (c)]. This approach can keep a good balance in the representativeness of urban patches and ensuring the reliability of network analysis.

Totally, 128 (58.5% of the total number) urban patches are selected in JJJ, accounting for 95.7% of urban areas; 239 (21.3% of the total number) urban patches are selected in YRD, accounting for 90.2%; and 28 (45.9% of the total number) urban patches are selected in PRD, accounting for 99.0%. For the spatial distribution information of urban patches, see Supplementary Figs. S2–S4. These urban patches are indexed with unique IDs using the labeling method. The urban spatial extents of Guangzhou, Shenzhen, Dongguan, and Foshan are connected and represented by their capital letters "GSDF" in the subsequent content. These urban patches are referred to as the basic components in the following urban connectivity analysis.

2) Representing Spatial Connectivity Using VIIRS: We use the inverted NTL intensity to represent a continuous cost surface that simulates the accessibility of human activities; that is, places with smaller cost distance (higher light intensity) values are more accessible areas to human activities. The absence of light pixels (i.e., completely dark pixels) indicates no human activities and is denoted as an infinity that represents no connectivity. Urban patches are connected to one another primarily along low "terrain" pixels with low cost distances, similar to water flows downhill. Previously, an eight-connectivity spatial filter is applied to mitigate abnormal observations with interrupted completely dark pixels on contiguous lighted linear connections.

3) Generation of Spatial Connectivity Among Urban Patches: We develop an object-based least-cost model to find optimal routes with the minimum cost value through the cost surface derived from VIIRS. In this method, each patch is regarded as a polygonal object, and connectivity among urban patches should be calculated starting from their boundaries rather than the point feature as patch centroids. The links among urban patches comprise a set of spatial contiguous pixels. The intensity of each spatial connectivity is quantified by averaging the corresponding path's NTL values. Details about each step are presented in the following (see Fig. 3).

First, for an urban patch label set with N patches denoted as U_N, the corresponding boundary point sets are denoted as B_N. The specific detection process for each patch object is as follows. For an urban patch $U_n(n \in N)$, the location of one of its boundary points $b_p(x, y)$ is masked as the search start L_s. As Tobler enunciated, nearby things are more related than distant things [55]. We observe from the VIIRS NTL images that the connection paths of two cities are always based on the boundary that is closest to each other. Therefore, we first determine the search direction by removing internal and other boundary points.

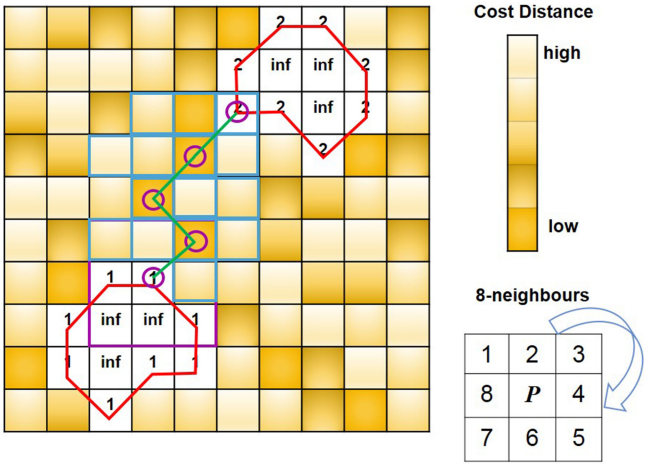

Fig. 3. Schematic of generating spatial connectivity among urban patches.

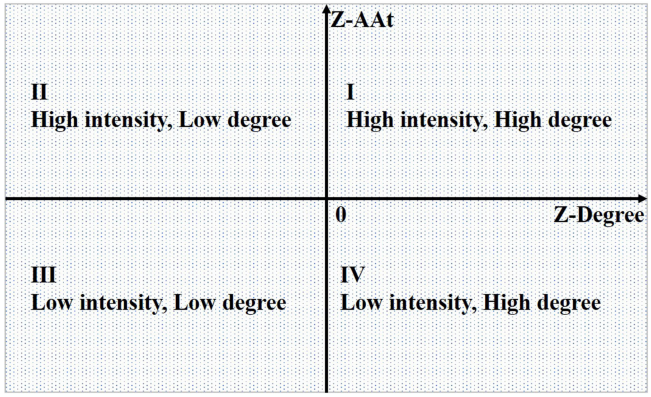

Fig. 4. Quadrant map of degree and average accessibility.

Then, we identify the link pixel-by-pixel and select the point where cost distance is the smallest in each step until the point value set in the next step contains other urban patch labeling ID values. The weights of paths among urban patches are measured by averaging NTL values located in paths. Duplicated paths are eliminated, and only the path with the highest NTL intensity is reserved to connect each patch pair.

B. Construction of Urban Spatial Connectivity Network

In this section, we construct a weighted and nondirectional spatial network in which the nodes (vertices) denote urban patches at the centroid of the patches, and the links (edges) represent the connectivity intensities of the links. Two nodes joined by a link are referred to as adjacent or neighboring. The number of links reflects the "connectedness" of the network. For a given number of nodes, more links indicate more close connectivity relationship among patches. Then, the network is abstracted as a mathematical representation, $G = (V,\ E)$, where $V = \{v_i,\ i = 1,\ 2,\ 3,\ \ldots, N\}$, $N = |V|$ is the number of nodes, and $E = \{e_i,\ i = 1,\ 2,\ 3,\ \ldots, M\}$, $M = |E|$ is the number of links. A binary $N \times N$ square adjacency (or connectivity) matrix, $\mathrm{Adj}(G)$, is created. It is a symmetric matrix to represent the network with entries $a_{ij} = 1\ (i \neq j)$ when a link exists between urban patch nodes i and j, and zero otherwise. The diagonal of the adjacency matrix contains zeros. The weighted network is generated by appending a weight to the corresponding link, and it can be described as $W\mathrm{Adj} = \{a_{ij} \times w_{ij}\}$. The weight w_{ij} of an edge linking node i and node j represents the connectivity intensity between these two nodes, which is calculated by averaging NTL values located in paths.

C. Quantitative Analysis of Urban Spatial Connectivity Network

1) Structural Properties and Node Centrality Analyses: A set of properties are calculated to characterize the connectivity network based on the graph theory (see Table II). Five indices, namely, cumulative degree distribution ($P^c(k)$), mean degree ($\bar{D}$), average shortest path length (L), diameter (d), and clustering coefficient (CC), are selected to quantify the overall structure of network. $P^c(k)$ is the fraction of nodes with degrees greater than or equal to k and is calculated to delineate how the connectivity is distributed in UAs. The CC characterizes the local cohesiveness of the current node (corresponds to the local CC_i of node i), and the extent to which the nodes in the network are clustered together (corresponds to the global CC of the network). A large value of $\mathrm{CC}(i)$ indicates that the node forms a compact system with its neighbors. Four indices are defined to measure each node centrality, including degree (C_D), closeness (C_C), betweenness (C_B), and node strength (C_S). These measures, respectively, represent a node's advantage of being directly connected to others, being accessible to others, being the intermediary between others, and being a powerful influence on others. More detailed definitions are also available in the [56]–[60].

2) Accessibility Analysis: We define an index, average accessibility index (AAt) to compare the accessibility of core urban nodes [11] using the following equation:

$$\mathrm{AAt}\,(i) = \frac{C_S\,(i)}{C_D\,(i)} \tag{1}$$

where $i = 1, 2, \ldots, N$. N indicates the number of urban nodes in a UA, $C_S(i)$ represents the weighted connectivity of node i in the network, and $C_D(i)$ denotes the degree of node i.

To discover the connectivity patterns of urban patches, we investigate the relationship between average accessibility indexes (AAt) and degrees of urban patches using the quadrant map method, which has been used in studies [60], [61] to delineate the relationship between urbanization and economic development. In this article, AAt is adopted to indicate the average intensity level for a core city, and degree represents the connection number level. Normalization method is implemented, and it generates *Z-AAt* and *Z-Degree*. In Fig. 4, the x-axis represents the direct connection number (z-score), and the y-axis represents the average connectivity intensity (z-score).

TABLE II
DEFINITIONS OF PROPERTIES TO CHARACTERIZE THE URBAN CONNECTIVITY NETWORK

Properties	Definition	Usage
Degree (C_D)	$C_D(i) = \sum_{i,j \in N} a_{ij}$	Node centrality
	The number of links of node i shared with others.	
Closeness (C_C)	$C_C = \frac{N-1}{\sum_{i,j \in N} d_{ij}}$	
	d_{ij} is the minimum number of links between nodes i and j.	
Betweenness (C_B)	$C_B(i) = \sum_{m \neq n \neq i} \frac{Path(m,i,n)}{Path(m,n)}$	
	$Path(m,i,n)$ is the number of the shortest paths between nodes m and n that pass through node i, and $Path(m,n)$ is the number of all shortest paths between nodes m and n.	
Strength (C_S)	$C_S(i) = \sum_{j \in \Gamma_i} W_{ij}$	
	Γ_i is the neighbor set of node i	
Cumulative degree distribution $P^C(k)$	$P^C(k) = \sum_{k' \geq k} p(k')$	Network structure
	$P(k)$ is the fraction of nodes with degree k.	
Mean degree ($\overline{D}$)	$\overline{D} = \frac{2 \times M}{N}$	
Average shortest path length (L)	$L = \frac{1}{n(n-1)} \sum_{i,j \in N} d_{ij}$	
	n is the number of node pairs.	
Diameter (d)	The maximum value of all d_{ij}.	
Clustering coefficient (CC)	$CC(i) = \frac{e_i}{\frac{1}{2} C_D(i)(C_D(i)-1)}$	
	$CC = \frac{1}{N} \sum_{i \in N} CC(i)$	
	e_i is the actual number of links for node i.	

IV. RESULTS AND DISCUSSION

A. Spatial Patterns of Urban Spatial Connectivity Networks

The proposed framework successfully detects the spatial connectivity relationship between urban areas. First, the use of land use data for extracting urban built-up areas can avoid the problem of overestimated built-up areas from NTL imagery because of its booming effect in urban areas. The detected built-up areas well delineate urban boundaries. Second, the proposed method can effectively detect the connection within a city and between cities. Third, the network analysis method based on the graph theory can well express the spatial differences of urban connectivity relationship and the roles of cities that play in UAs, whereas the previous rank-size method can only describe the overall size distribution of urban areas in UAs. The proposed framework can effectively mitigate the issues in previous studies and can be easily transferred to other regions.

1) Analysis of Spatial Distribution Characteristics: The spatial distribution of connectivity relationship exhibits evident spatial variability inside UAs and some similarities across UAs (see Fig. 5). First, the close and complex connection structures are in the core areas, whereas single-tree connection structures are found across the vast hinterland of the UAs. The urban patches in the core areas of each UA connect together directly or indirectly, and like a "block" visually compared with the isolated patches without connections with others. Both of connection numbers for the 4 core city regions in JJJ and 16 core city regions in YRD account for more than half and even up to 66.7% in YRD. Isolated patches are located in the northern part of Hebei Province [see Fig. 5(a)] in JJJ and also in the western and southern regions of Anhui Province in YRD [see Fig. 5(b)]. Both of these two areas are acknowledged to have a relatively backward development [62], [63]. The link intensity is classified into five levels using the Jenks Natural Breaks method to represent the spatial connectivity characteristics.

Second, high-intensity connections are mostly aggregated in the core areas of the UAs, such as Beijing and Tianjin JJJ [see Fig. 5(a)], Shanghai, Nanjing, Suzhou, Wuxi, Changzhou, Zhenjiang, Yangzhou, Nantong, Hangzhou, Huzhou, Shaoxing, and Jiaxing in YRD [see Fig. 5(b)], and Guangzhou, Shenzhen, Foshan, Dongguan, Hong Kong, and Macau in PRD [see Fig. 5(c)]. The average link intensities in both Beijing and Tianjin regions range from 8 to 12 nW/cm^2/sr, which are higher than the overall average of JJJ (see Table III). Third, an evident hub–spoke structure exists in these networks, such as Beijing, Tianjin, and Tangshan as hubs in JJJ; Shanghai, Nanjing, and Hangzhou in YRD; and Guangzhou and Shenzhen in PRD. Notably, only one provincial capital, Hefei (capital of Anhui Province), has fewer connections than other provincial capitals and municipalities [see Fig. 5(b)]. Summarily, the results show the strong influencing power of core cities in each UA. However, the findings about the spatial variability of connectivity also imply the severe inequality of development at the regional level, because core cities may have absolute advantages in economy, manpower, and

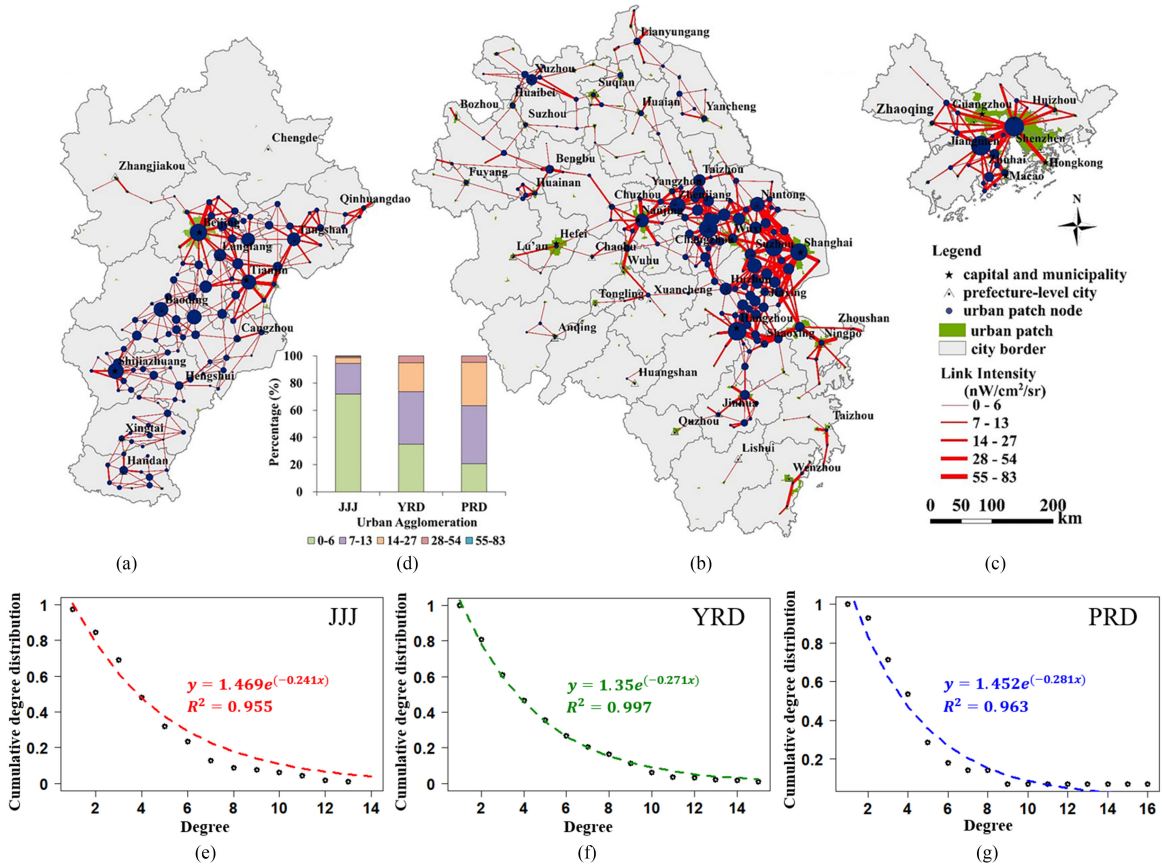

Fig. 5. Urban spatial connectivity networks: visualization of urban connectivity relationship (a)–(c), statistical distributions of connectivity levels (d), and cumulative distributions of node degrees (e)–(g). In the upper row, the size of a circle represents degree of this urban patch, and the thickness of lines denotes connectivity intensity. In panels (e)–(g), each scatter point represents the fraction of nodes with degrees greater than or equal to k (k is ranging from 1 to the maximum degree in an UA).

TABLE III
STATISTICS OF URBAN CONNECTIVITY NETWORKS

UA	Node	Link	Mean degree	Link intensity	Diameter	Average path length	Clustering coefficient	Isolate node percentage
JJJ	128	288	4.5	5.4	17	5.7	0.34	12/9.4%
YRD	239	461	3.9	10.7	23	8.0	0.39	18/7.5%
PRD	28	63	4.5	12.5	6	2.3	0.37	0

politics. The results demonstrate that this framework is effective for representing connectivity relationship of urbans in these three UAs.

2) Analysis of Statistics Characteristics: The cumulative distributions of degrees follow a power law distribution with an exponential relationship [see Fig. 5(e)–(g)]. It demonstrates the scale-free properties of the derived networks for these UAs that are similar as most networks in reality [56], [64]–[67] and indicates the presence of highly inhomogeneous distributions inside these networks. Actually, the distribution lead to the simultaneous presence of a few urban patches linking to many others as hubs and many poorly connected urban patches [57]. The findings are consistent with the visualized results (hub–spoke structures and isolated nodes) presented in Fig. 5(a)–(c).

Although there are many similar characteristics of connectivity networks as above among UAs, the levels of UA development still differ. The basic statistics results illustrate that YRD has the largest number of urban plates, whereas PRD has the most closely connected relationship among urban plates [see Fig. 5(d) and Table III]. Compared with each other, PRD is a well-connected network and accounts for more high-intensity connection ratios with the highest connectivity intensity in terms of overall network. Both JJJ and YRD have disconnected components and more low-intensity connection ratios. The average path lengths and diameters of the networks are proportional to the size (N) of the UAs. The clustering coefficients are approximately 0.3. It should be noted that there is a scale effect when comparing three UAs directly, especially considering their differences in spatial extents and numbers of urban patches,

TABLE IV
SPATIAL DISTRIBUTIONS OF HIGH-INTENSITY CONNECTIONS

Class	Link		UA
first (55–83)	Beijing–Shunyi[#]		JJJ
second (28–54)	Beijing–Huairou[#]	Tianjin–Binhai New District[#]	JJJ
	Shanghai–Kunshan	Shanghai–Pudong New District[#]	YRD
	Shanghai–Qingpu[#]	Shanghai–Songjiang[#]	
	Suzhou–Wujiang	Hangzhou–Xiaoshan[#]	
	Hangzhou–Yuhang[#]	Nantong–Changshu	
	Nantong–Taicang	Nanjing–Jiangning[#]	
	Ningbo–Cixi	Jiangyin–Zhangjiagang	
	Bengbu–Huaiyuan County[#]		
	GSDF–Hongkong	GSDF–Panyu	PRD

[#]District or county is subordinate to the city. GSDF is the acronym for Guangzhou, Shenzhen, Dongguan, and Foshan, which comprise the largest contiguous urban area in PRD. The division of these two high-intensity connections is following the classification presented in Fig. 5.

which can affect the overall analysis to a certain extent. For example, the smaller area of PRD and the spatially integrated development of many cities in PRD can lead to a higher average connectivity relationship of urban patches compared with JJJ and YRD. However, our results can still effectively reveal the high-level development of PRD from both of the high-connectivity characteristics and the fully connected network property according to the overall statistics [see Fig. 5(d) and Table III] and the local visualization details [see Fig. 5(a)–(c)], respectively, which is consistent with previous studies [68], [69].

3) Spatial Distributions of High-Intensity Connections: The spatial patterns of high-intensity connections at the top two levels show that high-intensity connections are concentrated in linking the core urban area of a city and its remote suburbs (see Table IV). For example, the core urban patch of Beijing has the highest intensity connection with its Shunyi District. Besides, the average intensity of the core urban patch with other urban patches in Beijing region is as high as 37.1 nW/cm^2/sr, followed by Shunyi of 29.9 nW/cm^2/sr, and both of those are far above the average intensity in JJJ of 5.4 nW/cm^2/sr. The core urban area is acknowledged as the center of economy, politics, culture, and education with the strongest radiation and attraction abilities, whereas the high influence of Shunyi District may be caused by the seat of Beijing Capital International Airport. In the second class, the connections between the center area of a city and its subordinate regions occupy 11 out of 17, such as Beijing and Huairou, Shanghai and its districts (Pudong New District, Qingpu, Songjiang), Hangzhou and its districts (Xiaoshan and Yuhang), GSDF and Panyu. In a word, the satellite urban patches are the first to be affected by the development of the core urban patch, especially in the context of rapidly expanding for the first- and second-tier cities in China.

In addition, high-intensity connections exist in linking the neighboring urban patches, such as Shanghai and Kunshan, Nantong and Changshu. Results also reflect the radiation drive of Shanghai for these areas. For example, Kunshan is the northern gateway that connects Shanghai and other areas in YRD. Cixi is the northwest gateway of Ningbo that connects to Shanghai, and both the two cities belong to the Hangzhou Bay New Area of Ningbo, which has been the state-level economic and technological development zone since 2014 [70]. Taicang is the gateway area of Nantong connecting to Shanghai. The urban areas of Bengbu and Huaiyuan County are nearly developing into one based on the visual judgment from daytime remote sensing images at the same period. The highest-intensity connection in PRD is between GSDF and Hong Kong, both of which are the most developed regions in PRD.

TABLE V
TOP TEN URBAN PATCHES BY NODE CENTRALITY MEASURES IN JJJ

Rank	Degree (C_D)	Closeness (C_C)	Betweenness (C_B)	Strength (C_S)
1	Beijing	Tianjin	Tianjin	Beijing
2	Shijiazhuang	Binhai^D	Hengshui	Tianjin
3	Tianjin	Cangzhou	Cangzhou	Shunyi^D
4	Baoding	Wuqing^D	Jizhou	Binhai^D
5	Renqiu	Jinghai^D	Wuyi^C	Shijiazhuang
6	Tangshan	Jinnan^D	Nangong	Wuqing^D
7	Baodi^D	Bazhou^D	Wuqing^D	Tangshan
8	Langfang	Wuyi^C	Dacheng^C	Sanhe
9	Bazhou	Baodi^D	Beijing	Huairou^D
10	Wuqing^D	Hengshui	Weixian^C	Baodi^D

Note: "D" and "C" in the upper right represent district and county, respectively.

TABLE VI
TOP TEN URBAN PATCHES BY NODE CENTRALITY MEASURES IN YRD

Rank	Degree (C_D)	Closeness (C_C)	Betweenness (C_B)	Strength (C_S)
1	Hangzhou	Zhenjiang	Zhenjiang	Shanghai
2	Changzhou	Danyang	Nanjing	Kunshan
3	Shanghai	Jiangyin	Changzhou	Hangzhou
4	Kunshan	Zhangjiagang	Cixi	Nantong
5	Zhenjiang	Nanjing	Suzhou	Suzhou
6	Nantong	Shanghai	Wuxi	Nanjing
7	Wujiang^D	Nantong	Danyang	Changzhou
8	Nanjing	Wujiang^D	Kunshan	Zhangjiagang
9	Changshu	Taicang	Bengbu	Zhenjiang
10	Zhangjiagang	Changshu	Chuzhou	Wujiang^D

Note: "D" and "C" in the upper right represent district and county, respectively

B. Node Centralities of Urban Patches

Core cities show higher centrality characteristics compared with other cities and play different roles in UAs (see Tables V–VII). For example, in JJJ, Beijing and Tianjin play two different roles, respectively (see Table V). Beijing as the leading city in JJJ is a highly attractive and inclusive city and holds powerful influence for other urban areas, ranking first both in degree and node strength; whereas Tianjin plays a bridging role between urbans and is closer to other patches, ranking first in both betweenness and closeness. Shanghai ranks first in strength as the leading city in YRD, Hangzhou ranks first in degree, whereas Zhenjiang ranks first in both betweenness and closeness (see Table VI). Differently, the largest contiguous urban plaque GSDF is ranked at the top in all indices, indicating its distinctive advantages in PRD (see Table VII). Results show core cities in JJJ and YRD play only part of roles, whereas the integrated area

TABLE VII
TOP TEN URBAN PATCHES BY NODE CENTRALITY MEASURES IN PRD

Rank	Degree (C_D)	Closeness (C_C)	Betweenness (C_B)	Strength (C_S)
1	GSDF	GSDF	GSDF	GSDF
2	FJZ	FJZ	FJZ	FJZ
3	Zhongshan	Zhongshan	Zhongshan	Zhongshan
4	Doumen^D	Hong Kong	Sihui	Panyu^D
5	ZM	Panyu^D	Doumen^D	Doumen^D
6	Foshan	Conghua	Guangning^C	ZM
7	Sihui	Foshan	Huizhou	Foshan
8	Panyu^D	Huizhou	ZM	Huizhou
9	Zengcheng^D	Zengcheng^D		Sihui
10	Zhaoqing	Boluo^C		Hong Kong

Note: "D" and "C" in the upper right represent district and county, respectively. GSDF is the acronym for Guangzhou, Shenzhen, Dongguan, and Foshan, which comprise the largest contiguous urban area in PRD. FJZ is the junction area of Foshan, Jiangmen, and Zhongshan, which comprise the second largest contiguous urban area in PRD. ZM is the acronym for Zhuhai and Macau.

of Guangzhou and Shenzhen regions is the definite dominance of all in PRD.

In terms of the measure of degree (C_D), Beijing is followed by Shijiazhuang, Tianjin, Baoding, and Renqiu, which are located in the central Hebei Province. Only Tianjin makes the top five in all the indices. Shijiazhuang, as the capital of Hebei Province, ranks only 49th in closeness and 11th in betweenness. Cangzhou ranks third in closeness and betweenness, and it may serve as an important transfer hub that connects Tianjin and cities in central Hebei Province. Notably, five districts of Tianjin appear in the top ten for closeness, namely, Binhai New District, Wuqing, Jinghai, Jinnan, and Wuyi. Shunyi ranks third in strength because of its advantage as an excellent air transportation center.

For YRD, the top ten of all indices in the list are the core areas of the YRD, except for Bengbu and Chuzhou. Bengbu and Chuzhou rank ninth and tenth, respectively, in betweenness. The former is a transportation hub in northern Anhui Province, and the latter is the gateway from Nanjing to northern Anhui. Furthermore, Nanjing as a gateway from core areas to peripheral regions, such as Anhui Province, ranks second in betweenness, only fifth in closeness, sixth in strength, and eighth in degree. Zhenjiang ranks first in closeness and betweenness. It also appears in the top ten in terms of degree and strength. Kunshan follows Shanghai in degree and strength given that it is the gateway of Shanghai to the north. Summarily, cites in Jiangsu province play more intensive relationship with each other than those of them in Zhejiang Province and Anhui Province.

In PRD, the urban hierarchical relationship is more discernable than the former two. Apart from the absolute influence of GSDF, the urban areas of FJZ and Zhongshan rank at the following top two regarding all indices (see Table VII). When sorted by the index of degree, Doumen District in Zhuhai, the urban plaque of Zhuhai and Macau, and Foshan rank at the fourth, fifth, and sixth, respectively. Doumen District ranks fifth in betweenness and strength. Several urban patches in peripheral regions, such as Sihui and Guangning County, also appear in the top ten list for betweenness. Panyu and Zengcheng Districts in Guangzhou are ranked in the top ten in terms of degree.

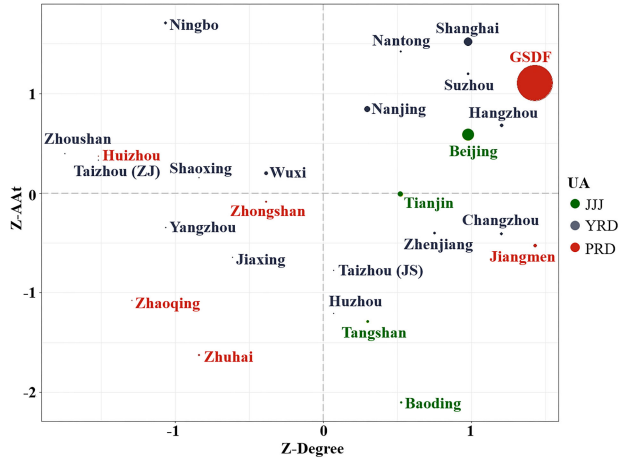

Fig. 6. Scatterplot of Z-degree and Z-AAt for core cities in the UAs. Circle sizes represent areas of urban patches. Taizhou (ZJ) represents the city belongs to Zhejiang Province, whereas Taizhou (JS) represents the city belongs to Jiangsu Province.

C. Node Accessibility of Urban Patches

The core cities show different connectivity patterns by mapping into a quadrant panel (see Fig. 6), and the result shows that the leading cities in each UA, namely, Shanghai, Beijing, and GSDF, have double-high levels of connection and connectivity intensity (Quadrant I). This finding indicates their absolute controlling role and radiative influence. Furthermore, Nantong and Suzhou in Jiangsu Province also exhibit double-high levels, followed by provincial capitals Hangzhou and Nanjing.

Approximately seven-eighths of the core cities in YRD have high levels of connections or connectivity intensity or both. Several cities are less connected but served as high-accessibility hubs. These cities include Ningbo, Taizhou, Wuxi, Zhoushan, and Shaoxing (Quadrant II). In contrast, fewer core cities (one-eighth) are located in the double-low level quadrant III. All cities in JJJ, excluding Beijing, are scattered in Quadrant IV, which are highly connected but have low connectivity intensity levels. For PRD, however, half of the cities are in the third quadrant with double-low levels. In addition, Ningbo in YRD has the highest connectivity intensity. GSDF and Jiangmen in PRD have the most connections.

V. CONCLUSION AND FUTURE WORK

In this article, we develop an object-based framework to investigate the connectivity relationship of urban areas using NTL observations and urban land use data. Urban areas are clustered, and the NTL data are represented as a continuous cost surface for human activities. The connections of urban patches occur along the low-cost distances, similar to water flow. Thereafter, the urban connectivity relationship is expressed as networks, and a graph-based method is used to analyze network structural properties and centralities of individual urban patches. We apply the proposed framework in three representative UAs in China. This article confirms the potential usage of NTL data, which can well capture urban connectivity relationship, as depicted by the spatial pattern and network analysis. The proposed approach can

detect the relationship of urban patches and has great potential to be applied at national and continental scales.

Conclusions are summarized from several aspects.

1) These networks exhibit the scale-free properties from the structural analysis, indicating the definite hub–spoke structures with core cities as hubs in each UA, and single-tree connection structures are observed across the vast hinterland of UAs.
2) Concentrated distribution of high connections is in the core areas of UAs. Connections at the top levels mainly link the urban areas of core cities and their remote suburbs in each UA.
3) The role of leading cities in each UA is different. Beijing holds both the highest degree and strength, whereas Tianjin has the highest closeness and betweenness in JJJ. In YRD, Hangzhou has the highest degree, whereas Shanghai has the highest strength, and Zhenjiang has the highest closeness and betweeness. GSDF ranks first in all centrality indices in PRD.
4) The quadrant map analysis discloses various connectivity patterns for core cities; Shanghai, Beijing, and GSDF have absolute advantages compared with other cities of UAs, with double-high levels of connections and average intensities.
5) The findings in this work indicate the mature development phase of PRD, followed by YRD, and finally JJJ.

The resulting urban connectivity networks derived from NTL observations can serve as essential information for analyzing the development of UAs. Especially in the context that the development of UA has become the trend of global urbanization. On November 18, 2018, the Chinese government issued a new statement that re-emphasized regional development strategy from two aspects: driving UA developments with leading cities, and driving regional development with UAs [70]. The results complement our knowledge of urban systems from statistical dataset and provide an effective understanding of spatial configurations of UAs. Findings also reveal the severe regional inequality, which can be useful for urban studies in line with sustainable development goals. Although NTL data provide an effective way to represent the spatial connectivity relationship of urban areas [43], the relationship of cities is complicated. The combination of NTL data and other multisource data, such as transportation, population, and social media data, is the trend of future research to explore the relationship of cities from a comprehensive perspective. In addition, with the increasingly archived NTL observations, the evaluation of urban connectivity dynamics is possible, which will be helpful in recognizing the evolution of intercity relations and UA development in future.

ACKNOWLEDGMENT

The VIIRS nighttime light data was downloaded from NOAA, https://ngdc.noaa.gov/eog/viirs/download_dnb_composites.html and the land use data was downloaded from http://www.resdc.cn/.

REFERENCES

[1] K. H. Zhang and S. Song, "Rural–urban migration and urbanization in China: Evidence from time-series and cross-section analyses," *China Econ. Rev.*, vol. 14, no. 4, pp. 386–400, 2003.
[2] C. He, Z. Liu, J. Tian, and Q. Ma, "Urban expansion dynamics and natural habitat loss in China: A multiscale landscape perspective," *Global Change Biol.*, vol. 20, no. 9, pp. 2886–2902, Sep. 2014.
[3] R. Lee, "The outlook for population growth," *Science*, vol. 333, no. 6042, pp. 569–573, 2011.
[4] J. Lin, Z. Wu, and X. Li, "Measuring inter-city connectivity in an urban agglomeration based on multi-source data," *Int. J. Geogr. Inf. Sci.*, vol. 33, no. 5, pp. 1062–1081, 2019.
[5] W. Loibl, G. Etminan, E. Gebetsroither-Geringer, H. M. Neumann, and S. Sanchez-Guzman, "Characteristics of urban agglomerations in different continents: History, patterns, dynamics, drivers and trends," in *Urban Agglomeration*. London, UK: IntechOpen, 2018, pp. 29–63.
[6] S. Heeg, B. Klagge, and J. OssenbruÜGge, "Metropolitan cooperation in Europe: Theoretical issues and perspectives for urban networking 1," *Eur. Planning Stud.*, vol. 11, no. 2, pp. 139–153, 2003.
[7] P. J. Taylor and R. Aranya, "A global 'Urban Roller Coaster'? Connectivity changes in the World City network, 2000–2004," *Reg. Stud.*, vol. 42, no. 1, pp. 1–16, 2008.
[8] L. Lu and R. Huang, "Urban hierarchy of innovation capability and inter-city linkages of knowledge in post-reform China," *Chin. Geogr. Sci.*, vol. 22, no. 5, pp. 602–616, 2012.
[9] R. Guimera, S. Mossa, A. Turtschi, and L. A. Amaral, "The worldwide air transportation network: Anomalous centrality, community structure, and cities' global roles," *Proc. Natl. Acad. Sci. USA*, vol. 102, no. 22, pp. 7794–7799, May 31, 2005.
[10] W.-B. Du, B.-Y. Liang, C. Hong, and O. Lordan, "Analysis of the Chinese provincial air transportation network," *Physica A*, vol. 465, pp. 579–586, 2017.
[11] S. Lu, Z. Fang, S. L. Shaw, and X. Zhang, "Impacts of high-speed rails on the accessibility inequality of railway network in China," in *Proc. 22nd IEEE Int. Conf. Geoinformat.*, 2014, vol. 1-5, pp. 1–5.
[12] A. De Montis, M. Barthélemy, A. Chessa, and A. Vespignani, "The structure of interurban traffic: a weighted network analysis," *Environ. Planning B, Planning Des.*, vol. 34, no. 5, pp. 905–924, 2007.
[13] A. Vasanen, "Functional polycentricity: Examining metropolitan spatial structure through the connectivity of urban sub-centres," *Urban Stud.*, vol. 49, no. 16, pp. 3627–3644, 2012.
[14] A. Belyi *et al.*, "Global multi-layer network of human mobility," *Int. J. Geogr. Inf. Sci.*, vol. 31, no. 7, pp. 1381–1402, Jul. 2017.
[15] M. R. Sanderson, B. Derudder, M. Timberlake, and F. Witlox, "Are world cities also world immigrant cities? An international, cross-city analysis of global centrality and immigration," *Int. J. Comparative Sociol.*, vol. 56, no. 3-4, pp. 173–197, 2015.
[16] Y. Liu, Z. Sui, C. Kang, and Y. Gao, "Uncovering patterns of inter-urban trip and spatial interaction from social media check-in data," *PloS One*, vol. 9, no. 1, 2014, Art. no. e86026.
[17] L. F. Xiong, F. Zhen, B. Wang, and G. L. Xi, "The research of the Yangtze River Delta Core Area's City network characteristics based on Baidu index," *Econ. Geogr.*, vol. 33, no. 7, pp. 67–73, 2013.
[18] Z. Feng, W. Bo, and C. Yingxue, "China's City network characteristics based on social network space: An empirical analysis of Sina micro-blog," *Acta Geogr. Sin.*, vol. 67, no. 8, pp. 1031–1043, 2012.
[19] J. R. Jensen and D. C. Cowen, "Remote sensing of urban/suburban infrastructure and socio-economic attributes," *Photogramm. Eng. Remote Sens.*, vol. 65, pp. 611–622, 1999.
[20] X. Liu *et al.*, "High-resolution multi-temporal mapping of global urban land using Landsat images based on the Google earth engine platform," *Remote Sens. Environ.*, vol. 209, pp. 227–239, 2018.
[21] Y. Zhou, X. Li, G. R. Asrar, S. J. Smith, and M. Imhoff, "A global record of annual urban dynamics (1992–2013) from nighttime lights," *Remote Sens. Environ.*, vol. 219, pp. 206–220, 2018.
[22] M. Zhao *et al.*, "Applications of satellite remote sensing of nighttime light observations: Advances, challenges, and perspectives," *Remote Sens.*, vol. 11, no. 17, 2019, Art. no. 1971.
[23] X. Li and Y. Zhou, "Urban mapping using DMSP/OLS stable night-time light: A review," *Int. J. Remote Sens.*, vol. 38, no. 21, pp. 6030–6046, 2017.
[24] X. Li *et al.*, "Anisotropic characteristic of artificial light at night—Systematic investigation with VIIRS DNB multi-temporal observations," *Remote Sens. Environ.* vol. 233, 2019, Art. no. 111357.

[25] S. Keola, M. Andersson, and O. Hall, "Monitoring economic development from space: Using nighttime light and land cover data to measure economic growth," *World Dev.*, vol. 66, pp. 322–334, 2015.
[26] P. C. Sutton, C. D. Elvidge, and T. Ghosh, "Estimation of gross domestic product at sub-national scales using nighttime satellite imagery," *Int. J. Ecol. Econ. Statist.*, vol. 8, no. S07, pp. 5–21, 2007.
[27] X. Li, H. Xu, X. Chen, and C. Li, "Potential of NPP-VIIRS nighttime light imagery for modeling the regional economy of China," *Remote Sens.*, vol. 5, no. 6, pp. 3057–3081, 2013.
[28] C. Yang *et al.*, "A spatial-socioeconomic urban development status curve from NPP-VIIRS nighttime light data," *Remote Sens.*, vol. 11, no. 20, 2019, Art. no. 2398.
[29] H. Bagan and Y. Yamagata, "Analysis of urban growth and estimating population density using satellite images of nighttime lights and land-use and population data," *GISci. Remote Sens.*, vol. 52, no. 6, pp. 765–780, 2015.
[30] D. Li, X. Zhao, and X. Li, "Remote sensing of human beings—A perspective from nighttime light," *Geospatial Inf. Sci.*, vol. 19, no. 1, pp. 69–79, 2016.
[31] L. Zhuo, T. Ichinose, J. Zheng, J. Chen, P. J. Shi, and X. Li, "Modelling the population density of China at the pixel level based on DMSP/OLS non-radiance-calibrated night-time light images," *Int. J. Remote Sens.*, vol. 30, no. 4, pp. 1003–1018, 2009.
[32] K. Shi *et al.*, "Spatiotemporal variations of CO_2 emissions and their impact factors in China: A comparative analysis between the provincial and prefectural levels," *Appl. Energy*, vol. 233/234, pp. 170–181, 2019.
[33] J. Tian, N. Zhao, E. L. Samson, and S. Wang, "Brightness of nighttime lights as a proxy for freight traffic: A case study of China," *IEEE J. Sel. Topics Appl. Earth Observ. Remote Sens.*, vol. 7, no. 1, pp. 206–212, Jan. 2014.
[34] K. Shi *et al.*, "Modeling and mapping total freight traffic in China using NPP-VIIRS nighttime light composite data," *GISci. Remote Sens.*, vol. 52, no. 3, pp. 274–289, 2015.
[35] Q. Zhang and K. C. Seto, "Mapping urbanization dynamics at regional and global scales using multi-temporal DMSP/OLS nighttime light data," *Remote Sens. Environ.*, vol. 115, no. 9, pp. 2320–2329, 2011.
[36] R. C. Sharma, R. Tateishi, K. Hara, S. Gharechelou, and K. Iizuka, "Global mapping of urban built-up areas of year 2014 by combining MODIS multispectral data with VIIRS nighttime light data," *Int. J. Digit. Earth*, vol. 9, no. 10, pp. 1004–1020, 2016.
[37] T. Ma, C. Zhou, T. Pei, S. Haynie, and J. Fan, "Quantitative estimation of urbanization dynamics using time series of DMSP/OLS nighttime light data: A comparative case study from China's cities," *Remote Sens. Environ.*, vol. 124, pp. 99–107, 2012.
[38] Y. Zhou *et al.*, "A global map of urban extent from nightlights," *Environ. Res. Lett.*, vol. 10, no. 5, 2015, Art. no. 054011.
[39] Z. Q. Chen *et al.*, "Mapping global Urban areas from 2000 to 2012 using time-series nighttime light data and MODIS products," *IEEE J. Sel. Top. Appl. Earth Observ.*, vol. 12, no. 4, pp. 1143–1153, Apr. 2019.
[40] B. L. Yu *et al.*, "Object-based spatial cluster analysis of urban landscape pattern using nighttime light satellite images: A case study of China," *Int. J. Geogr. Inf. Sci.*, vol. 28, no. 11, pp. 2328–2355, 2014.
[41] Z. Q. Chen *et al.*, "A new approach for detecting urban centers and their spatial structure with nighttime light remote sensing," *IEEE Trans. Geosci. Remote Sens.*, vol. 55, no. 11, pp. 6305–6319, Nov. 2017.
[42] B. Wu, B. Yu, S. Yao, Q. Wu, Z. Chen, and J. Wu, "A surface network based method for studying urban hierarchies by night time light remote sensing data," *Int. J. Geogr. Inf. Sci.*, vol. 33, pp. 1377–1398, 2019.
[43] C. Small, C. D. Elvidge, and K. Baugh, "Mapping urban structure and spatial connectivity with VIIRS and OLS night light imagery," in *Proc. IEEE Joint Urban Remote Sens. Event*, 2013, pp. 230–233.
[44] C. Small, C. D. Elvidge, D. Balk, and M. Montgomery, "Spatial scaling of stable night lights," *Remote Sens. Environ.*, vol. 115, no. 2, pp. 269–280, 2011.
[45] C. Small, F. Pozzi, and C. Elvidge, "Spatial analysis of global urban extent from DMSP-OLS night lights," *Remote Sens. Environ.*, vol. 96, no. 3/4, pp. 277–291, 2005.
[46] China Administrative Division Data Set. Accessed: Feb. 9, 2020. [Online]. Available: http://www.resdc.cn/.
[47] S. M. Yao, C. S. Zhou, D. Wang, C. L. Xiu, C. X. Wang, and M. X. Chen, *New Perspectives on Urban Agglomerations in China*. Beijing, China: Science Press, 2016, pp. 185–257. (in Chinese).
[48] Statistical Yearbook of China. 2016. Accessed: Jan. 2, 2019. [Online]. Available: http://www.stats.gov.cn/tjsj/ndsj/2016/indexch.htm.
[49] VIIRS Data Set. Accessed: Dec. 5, 2018. [Online]. Available: https://ngdc.noaa.gov/eog/viirs/download_dnb_composites.html
[50] X. Zhao, D. Li, X. Li, L. Zhao, and C. Wu, "Spatial and seasonal patterns of night-time lights in global ocean derived from VIIRS DNB images," *Int. J. Remote Sens.*, vol. 39, no. 22, pp. 8151–8181, 2018.
[51] Land Use Data Set. Accessed: Dec. 5, 2018. [Online]. Available: http://www.resdc.cn/.
[52] Z. Liu, C. He, Q. Zhang, Q. Huang, and Y. Yang, "Extracting the dynamics of urban expansion in China using DMSP-OLS nighttime light data from 1992 to 2008," *Landscape Urban Planning*, vol. 106, no. 1, pp. 62–72, 2012.
[53] Y. Zhou, S. J. Smith, C. D. Elvidge, K. Zhao, A. Thomson, and M. Imhoff, "A cluster-based method to map urban area from DMSP/OLS nightlights," *Remote Sens. Environ.*, vol. 147, pp. 173–185, 2014.
[54] L. De Cola, "A network representation of raster land-cover patches," *Photogramm. Eng. Remote Sens.*, vol. 76, no. 1, pp. 61–72, 2010.
[55] H. J. Miller, "Tobler's first law and spatial analysis," *Ann. Assoc. Amer. Geogr.*, vol. 94, no. 2, pp. 284–289, 2004.
[56] T. Jia and B. Jiang, "Building and analyzing the US airport network based on en-route location information," *Physica A*, vol. 391, no. 15, pp. 4031–4042, 2012.
[57] S. Boccaletti, V. Latora, Y. Moreno, M. Chavez, and D. Hwang, "Complex networks: Structure and dynamics," *Phys. Rep.*, vol. 424, no. 4-5, pp. 175–308, 2006.
[58] P. Galpern, M. Manseau, and A. Fall, "Patch-based graphs of landscape connectivity: A guide to construction, analysis and application for conservation," *Biol. Conserv.*, vol. 144, no. 1, pp. 44–55, 2011.
[59] A. Barrat, M. Barthelemy, R. Pastor-Satorras, and A. Vespignani, "The architecture of complex weighted networks," *Proc. Natl. Acad. Sci. USA.*, vol. 101, no. 11, pp. 3747–3752, Mar. 2004.
[60] M. X. Chen, D. D. Lu, and L. S. Zha, "Urbanization and economic development in China: An international comparison based on quadrant map approach," *Geographical Res.*, vol. 26, no. 2, pp. 25–34, 2009.
[61] H. Fu, Z. Shao, P. Fu, and Q. Cheng, "The dynamic analysis between urban nighttime economy and urbanization using the DMSP/OLS nighttime light data in China from 1992 to 2012," *Remote Sens*., vol. 9, no. 5, 2017, Art. no. 416.
[62] S. J. Wang, H. Ma, and Y. B. Zhao, "Exploring the relationship between urbanization and the eco-environment—A case study of Beijing–Tianjin–Hebei region," *Ecol. Indicators*, vol. 45, pp. 171–183, 2014.
[63] J. L. Zhou, *Anhui Province City Development Report*. Hefei, China: Hefei Univ. Technol. Press, 2016.
[64] L. A. Adamic and B. A. Huberman, "Power-law distribution of the world wide web," *Science*, vol. 287, no. 5461, pp. 2115–2115, 2000.
[65] S. H. Strogatz, "Exploring complex networks," *Nature*, vol. 410, no. 6825, pp. 268–276, 2001.
[66] A. L. Barabasi and Z. N. Oltvai, "Network biology: Understanding the cell's functional organization," *Nat. Rev. Genet.*, vol. 5, no. 2, pp. 101–113, 2004.
[67] M. Barthélemy, "Spatial networks," *Phys. Rep.*, vol. 499, no. 1/3, pp. 1–101, 2011.
[68] X. L. Gao, Z. N. Xu, F. Q. Niu, and Y. Long, "An evaluation of China's urban agglomeration development from the spatial perspective," *Spat. Statist.*, vol. 21, pp. 475–491, 2017.
[69] The Development Report of Chinese Urban Agglomerations. Accessed: Feb. 15, 2020. [Online]. Available: https://www.cdrf.org.cn/jjhdt/4898.jhtml
[70] China National Economic and Technological Development Zone. Ministry of Commerce of the People's Republic of China. Accessed: Jan. 2, 2019. [Online]. Available: http://www.mofcom.gov.cn/xglj/kaifaqu.shtml

Xia Zhao received the B.S. degree in geographic information system from the China University of Petroleum (Huadong), Qingdao, China, in 2014. She is currently working toward the Ph.D. degree in photogrammetry and remote sensing with the State Key Laboratory of Information Engineering in Surveying, Mapping and Remote Sensing (LIESMARS), Wuhan University, Wuhan, China.

She is a Visiting Student with the Department of Geological and Atmospheric Sciences, Iowa State University, Ames, IA, USA. Her research interests include night-time light remote sensing, spatial data mining, urbanization, and its potential environmental impacts.

Xi Li received the Ph.D. degree in photogrammetry and remote sensing from Wuhan University, Wuhan, China, in 2009.

He is an Associate Professor with the State Key Laboratory of Information Engineering in Surveying, Mapping and Remote Sensing (LIESMARS), Wuhan University. His research interests include physical modeling of night-time light as well as night-time light remote sensing applications.

Dr. Li is an Editorial Board Member of *International Journal of Remote Sensing* and an International Consultant for Asian Development Bank.

Yuyu Zhou received the B.S. degree in geography and the M.S. degree in remote sensing from Beijing Normal University, Beijing, China, in 2001 and 2004, respectively, and the Ph.D. degree in environmental sciences from the University of Rhode Island, Kingston, RI, USA, in 2008.

He is an Associate Professor with the Department of Geological and Atmospheric Sciences, Iowa State University, Ames, IA, USA. His research interests include applications of remote sensing, geographic information systems, integrated assessment modeling, and spatial analysis to understand the problems of environmental change and their potential solutions.

Deren Li received the Doctoral degree from the University of Stuttgart, Stuttgart, Germany, in 1985, and the Honorary Doctorate from ETH Zürich, Switzerland, in 2008.

He is currently a Professor with the Laboratory of Information Engineering in Surveying, Mapping and Remote Sensing (LIESMARS), and the Director of the Collaborative Innovation Center of Geospatial Technology, at Wuhan University, Wuhan, China. Highlights of his many achievements are the design of ZY-3, the first Chinese mapping satellite used to produce 1:50.000 orthophotos and digital surface models for large area (1000–2500 km^2) without ground control points. Collaborating with Prof. Jianya Gong, he further developed the three generations of GIS software, GeoStar, GeoGlobe, and GeoSmart, which have been widely used for the construction of digital cities and smart cities in China and beyond. He was also instrumental in introducing the integration of theories and algorithms of global navigation satellite systems, remote sensing and geographic information systems, which support such diverse applications as mobile mapping, unmanned aerial vehicle systems and many others. He has authored/coauthored eight books and more than 400 papers. His research interests include photogrammetry and remote sensing, global navigation satellite systems, and geographic information systems, and their innovation integrations and applications in China.

Dr. Li is a member of both the Chinese Academy of Sciences and the Chinese Academy of Engineering.